Environmental Pollution 311 (2022) 119964

Contents lists available at ScienceDirect

Environmental Pollution

journal homepage: www.elsevier.com/locate/envpol

Fuel from within: Can suspended phosphorus maintain algal blooms in Lake Dianchi☆

Zuxue Jin [a,b], Jingfu Wang [a,b,*], Shihao Jiang [a], Jiaojiao Yang [a,b], Shuoru Qiu [a,b], Jingan Chen [a,b]

[a] State Key Laboratory of Environmental Geochemistry, Institute of Geochemistry, Chinese Academy of Sciences, Guiyang, 550081, PR China
[b] University of Chinese Academy of Sciences, Beijing, 100049, PR China

ARTICLE INFO

Keywords:
Phosphorus speciation
Solution phosphorus-31 nuclear magnetic resonance (^{31}P NMR)
Chemical sequential extraction
Alkaline phosphatase

ABSTRACT

Extensive algal bloom in the surface water is a pressing issue in Lake Dianchi that causes lake restoration to be difficult owing to complex and variable phosphorus (P) sources in the water column. P released from algae, suspended particles (SS), and sediment can provide sustainable P sources for algal blooms. However, little is known regarding the dynamic of P speciation in these substances from different sources. In this study, solution ^{31}P nuclear magnetic resonance (^{31}P NMR) and chemical sequential extraction were employed to identify P speciation in algae, SS, and sediment during different periods. Results showed that dissolved inorganic P (P_i) directly accumulated in algae in the form of orthophosphate (ortho-P) and pyrophosphate (pyro-P). Algae preferentially utilized P_i, followed by organic P (P_o) in the water column when the P_i was insufficient during growth and reproduction. The ^{31}P NMR spectra demonstrated that ortho-P, orthophosphate monoesters (mono-P), orthophosphate diesters (diester-P), and pyro-P dominated the P compounds across the samples tested. Increasing remineralization of SS mono-P driven by intense alkaline phosphatase activities was caused by increasing P needs of algae and pressure of P supply in the water column. The higher ratios of diester-P to mono-P in sediment (mean 0.55) than those in algae (mean 0.07) and SS (mean 0.11 in surface water, 0.14 in bottom water) suggested that the degradation and regeneration occurred within these P compounds during or after sedimentation. P_i content in algae during growth and reproduction was controlled by its P absorption and utilization strategies. Results of this study provide insights into the dynamic cycling of P in algae, SS, and sediment, explaining the reason for algal blooms in the surface water with low concentrations of dissolved P.

1. Introduction

Lake Dianchi (102°36'−102°47′ E, 24°40'−25°02′ N) is a typical eutrophic lake in the Yunnan Province, southwest China. In the last 50 years, elevated nutrient loading in the lake has led to extensive algal blooms in the surface water (Ma et al., 2015; Wu et al., 2017; Xie et al., 2019; Zhang et al., 2020). The higher annual (1988–2018) average molar ratio of total nitrogen (TN) to total phosphorous (TP) compared to the Redfield ratio (e.g., 16 for N/P) (Gao et al., 2021) indicates that phosphorus (P) is the limiting nutrient in the lake. However, the sources, transformation, and cycling of P in the water column are more complicated than those of other nutrients, mainly because (1) soluble reactive P (SRP) concentrations are lower than those of TP in the water column; (2) the transformations of organic P (P_o) and inorganic P (P_i) in the water column are active and variable; and (3) P uptake and cycling strategies of organisms vary at different compositions and concentrations of P_o and P_i compounds. These complexities not only hinder the identification of P compounds and their transformation processes but also restrict the design of effective strategies for lake nutrient management.

The concentrations of TP in the water column of Lake Dianchi (0.1–0.2 mg L^{-1}) were 10 times greater than those of SRP (<0.01 mg L^{-1}) and dissolved P_o (<0.01 mg L^{-1}) (He et al., 2014; Wang et al., 2018). Furthermore, in the last 10 years, external P inputs to the Lake Dianchi watershed have been effectively controlled. However, algal blooms still occurred annually in the surface water of the lake (Bai et al., 2017; Wu et al., 2017; Feng et al., 2020). This can be attributed to the release of internal P (e.g., from suspended particles (SS), algae, and sediment) (Shinohara et al., 2012; Feng et al., 2020). Studies of internal

☆ This paper has been recommended for acceptance by Sarah Harmon.

* Corresponding author. State Key Laboratory of Environmental Geochemistry, Institute of Geochemistry, Chinese Academy of Sciences, Guiyang, 550081, PR China.
E-mail addresses: jinzuxue@mail.gyig.ac.cn (Z. Jin), wangjingfu@vip.skleg.cn (J. Wang).

https://doi.org/10.1016/j.envpol.2022.119964
Received 19 March 2022; Received in revised form 7 August 2022; Accepted 9 August 2022
Available online 22 August 2022

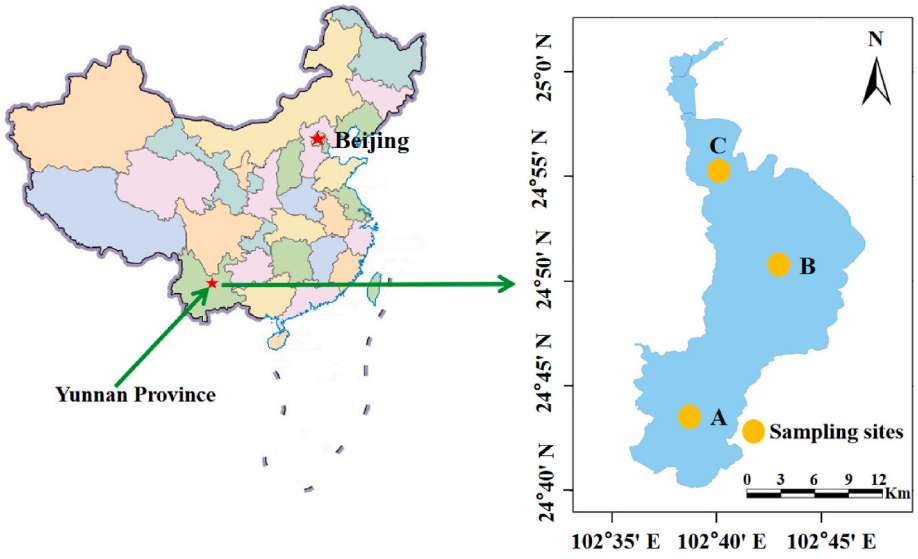

Fig. 1. Sampling sites. Sites A, B, and C are located in the south, middle, and north of the Lake Dianchi, respectively.

P in lakes have mainly focused on sediment P, such as the mechanisms driving sediment P release, P species, and P compounds (Zhu et al., 2013; Wu et al., 2017; Chen et al., 2018), whereas little is known about the P dynamic of SS and algae. Similar to sediment, SS and algae can also release P due to oxidation-reduction potential (ORP) changes and enzymes (Shinohara et al., 2012; Feng et al., 2020; Wang et al., 2021a). Therefore, identifying P compounds in SS, algae, and sediment is indispensable because these compounds collectively determine the mechanisms of P release (Zhu et al., 2013; Yang et al., 2020).

In this study, we hypothesized that P released from SS during or after sedimentation can provide an important P source for algal growth and reproduction. To test this, we combined solution ^{31}P NMR with chemical sequential extraction to identify and quantify the P speciation in algae, SS, and sediment. The objectives of this study were to (1) investigate the strategies of P absorption and utilization in algae; (2) identify the compositions and differences of P compounds from different substances; and (3) reveal the differences of bioavailable P in different substances. Results gained from this study provide important insights into the degradation and regeneration of P speciation in algae, SS, and sediment in response to algal blooms in the surface water where is low concentrations of dissolved P in the water column.

2. Materials and methods

2.1. Study sites

Lake Dianchi is the sixth largest lake in China, with a surface area of 330 km^2 and a mean depth of 5.0 m (Zhu et al., 2013; Wang et al., 2021b). Several rivers flow into the lake but there is only one outlet. Furthermore, the residence time of water is three to eight years, which accelerates the internal nutrient cycle in the water column. The water in the lake is completely mixed because of the subtropical monsoon climate and wind disturbances (Zhu et al., 2013; Wu et al., 2017). Sampling sites are shown in Fig. 1.

2.2. Sample collection, physicochemical properties, and preparation

SS, algae, and sediment were collected from the same sample sites in 2021 (January, April, and July). To obtain sufficient SS for P speciation analysis, a large volume of water (60 L) was collected from the surface water (0.5 m below surface water) and bottom water (0.5 m above sediment) using a Niskin sampler. SS were collected by filtrating lake water with precombusted (450 °C, 4 h) and preweighted glass-fiber filters (GF/F, 0.7 μm Whatman, UK) (note: one filter was used to filter 10 L of water). The filters were then stored in precombusted (450 °C for 4 h) aluminium foil (Yu et al., 2020). An additional 2 L of water was collected from the same sites (including surface water and bottom water), of which 1.5 L was used for algae abundance analysis after adding 3–5 mL of formaldehyde and another 0.5 L was used for physicochemical properties analysis. Algae (0.5 m below surface water) was collected by using a phytoplankton net (200 mesh, pore diameter 0.064 mm) (Feng et al., 2020) and stored in clean polyethylene bottles. Sediment core samples were obtained from the same sites by using a gravity core sampler, and surface sediment samples (0–2 cm) were collected by slicing the top of core and stored in centrifuge tubes. All samples were stored at 4 °C and immediately transferred into the laboratory for analysis. Water temperature (T), dissolved oxygen (DO), pH, and ORP were measured by using a multi-parameter water quality monitor (YSI6600–V2, YSI Co, USA). TP in water samples was digested with potassium persulfate and analyzed by using the molybdenum blue method (Huang et al., 1999). Algae abundance, water alkaline phosphatase activities, and SS concentrations were determined by optical microscopy counting, the p-nitrophenyl phosphate disodium colorimetric method, and the gravimetric method, respectively (Gage and Gorham., 1985; Boon, 1989; Hu and Wei., 2006; Ji et al., 2022). Algae samples were repeatedly and carefully washed with ultra-pure water and impurities were removed as much as possible (Feng et al., 2016; Feng et al., 2018) (Fig. S1). Algae, SS, and sediment samples were freeze-dried (−80 °C). Lyophilized algae and sediment were ground, sieved through a 200−mesh, and stored at −20 °C until analysis. Lyophilized SS were also stored at −20 °C until analysis.

2.3. ^{31}P NMR analysis

Solution ^{31}P NMR was used to identify the P compounds in the samples. Algae (0.2 g), sediment (2 g), and SS (SS from 40 L lake water collected on four glass-fiber filters) were extracted for 16 h using NaOH-EDTA (0.25 M NaOH and 50 mM EDTA) solution (40 mL) (Cade-Menun and Preston., 1996; Ahlgren et al., 2006; Doolette et al., 2009; Shinohara et al., 2012; Yang et al., 2020). After extraction, the samples were centrifuged at 14000 rpm (4 °C) for 15 min. Subsequently, the supernatants were filtered by glass-fiber filters (GF/F), and 1 mL of supernatants were collected to conduct triplicate TP contents. The method used for analyzing TP contents of the NaOH-EDTA extracts was identical to that used for the water samples. The filtrates were then freeze-dried for ^{31}P NMR measurement.

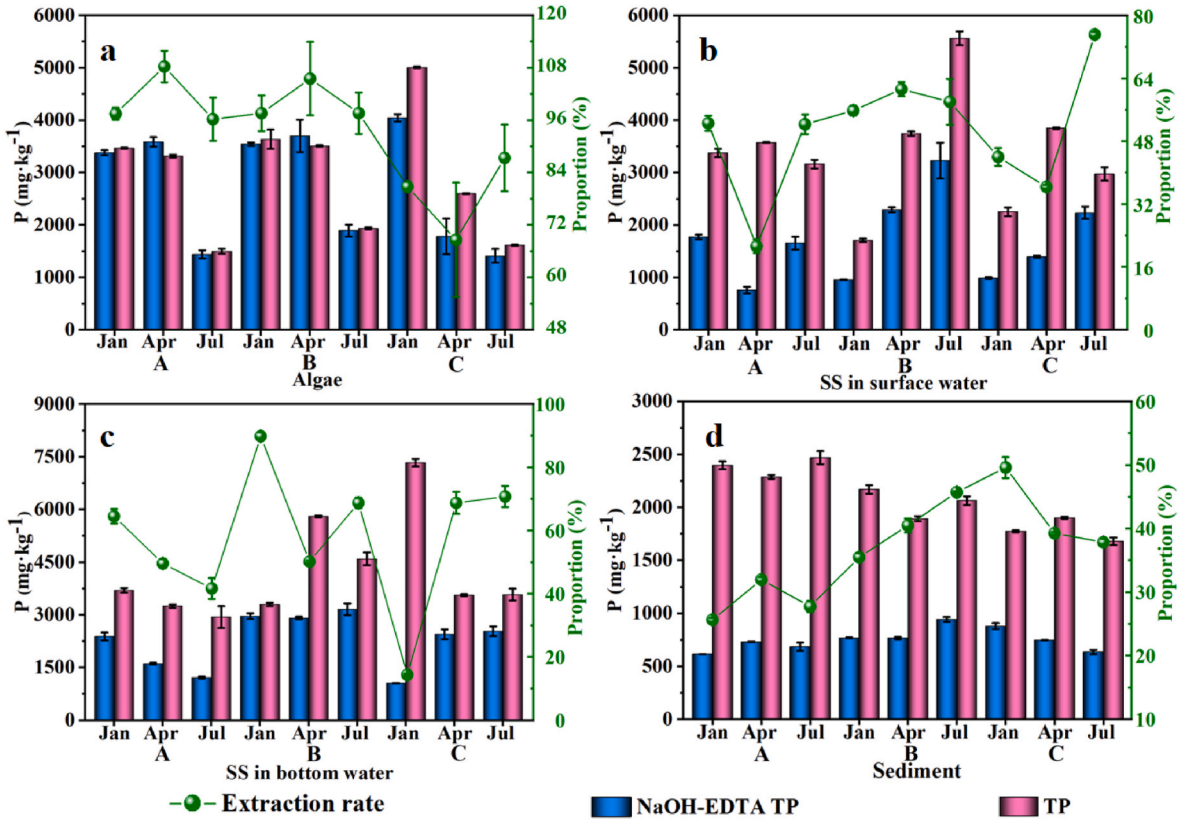

Fig. 2. Contents of TP, and NaOH-EDTA TP, and the extraction ratios of NaOH-EDTA TP (calculated as NaOH-EDTA TP/TP) in algae, suspended particles (SS), and sediment. Note: Panel a, b, c, and d represent algae, SS from surface water, SS from bottom water, and sediment, respectively. Error bar represents standard deviations of triplicated measurements. Where error bars are not visible, they are smaller than the data symbols.

Immediately before ^{31}P NMR analysis, the lyophilized powder was re-dissolved with 0.1 mL of 10 mol L^{-1} NaOH. Subsequently 0.6 mL D_2O was added to each sample to lock the signals. The samples were transferred into a 5 mm NMR tube. ^{31}P NMR spectra were obtained by using a Bruker Avance NEO 600 MHz NMR Spectrometer (Bruker Corporation, USA) operating at 129.5 Hz for ^{31}P. Other NMR parameters were 12.00 usec pulse, pulse 3.00 dB power, 2 s relaxation delay, 20,000 scans (10–15 h), and 20 °C. Chemical shifts were indirectly referenced an external standard (85% H_3PO_4, δ = 0 ppm, Tianjin Kemiou Chemical Reagent Co., Ltd, Tianjin, China) (Ahlgren et al., 2006; Li et al., 2015).

Peaks were identified by comparing with the chemical shifts from previous studies (Turner et al., 2003; Cade-Menun, 2005; Shinohara et al., 2012; Feng et al., 2018; Yang et al., 2020). Compared with previous findings (Cade-Menun, 2005; Yang et al., 2020), approximately 0.5 ppm difference was observed in this study. Each P compound had its corresponding chemical shift: orthophosphate (ortho-P, 5.5–7.0 ppm), orthophosphate monoesters (mono-P, 3.0–5.5 ppm), orthophosphate diesters (diester-P, −1.5–2.5 ppm), pyrophosphate (pyro-P, −3.0 to −5.0 ppm). The content of each P compound was calculated by multiplying its corresponding percentage of the ^{31}P NMR spectra with the contents of the corresponding NaOH-EDTA TP.

2.4. Analysis of P species in algae, suspended particles, and sediment

The P species in algae, SS, and sediment were analyzed by using the modified sequential extraction method (Hedley et al., 1982; Liu et al., 2019). Briefly, algae (0.2 g), SS (SS were collected from filtered 10 L lake water), and sediment (0.2 g) were sequentially extracted for 16 h using ultra-pure water, 0.5 M $NaHCO_3$ (pH = 8.50), 0.1 M NaOH, and 1 M HCl solution (solid:liquid = 1:60). These samples were centrifuged at 4390 g for 15 min after extraction, and the obtained supernatants were filtered through glass-fiber filters (GF/F). The P_i concentrations of the supernatants were determined by using the molybdenum blue method (Murphy and Riley, 1962). The combustion method (Aspila et al., 1976) was used to determine TP contents of algae (0.2 g), SS (SS were collected from filtered 10 L lake water), and sediment (0.2 g). P_o contents of algae, SS, and sediment were calculated based on the difference between TP and P_i (Tang et al., 2018; Yang et al., 2021). All samples were measured at least in triplicate.

3. Results

3.1. Physicochemical properties in water and the relationship between them

The water chemistry parameters are shown in Fig. S2−S4. Specifically, T, DO, ORP, and pH ranged from 11.0 to 24.3 °C, from 0.71 to 9.75 mg L^{-1}, from −177.0 to 172.0 mV, and from 7.25 to 9.39, respectively (Fig. S2). The concentrations of SS and TP ranged from 4.53 to 29.39 mg L^{-1} and from 0.07 to 0.20 mg L^{-1}, respectively (Fig. S3a, b). Alkaline phosphatase activities ranged from 6.24 to 50.34 nmol (L $min)^{-1}$ (Fig. S3c). Algae abundance ranged from 43 × 10^4 to 1800 × 10^4 cells L^{-1} (Fig. S4).

The correlations among water chemistry, P compounds, and P species in algae and SS (Pearson's correlation coefficients) are shown in Tables S1 - S2. Significant correlations were found among TP concentrations and DO, pH, and T in the water column (Table S1). A significant negative correlation was observed between alkaline phosphatase activities and TP concentrations in the water column (Table S1). TP concentration was positively correlated with H_2O-P_i, ortho-P, mono-P, diester-P, and pyro-P concentrations of algae (Table S1 - S2). Significant positive correlations were observed among ortho-P, mono-P, diester-P,

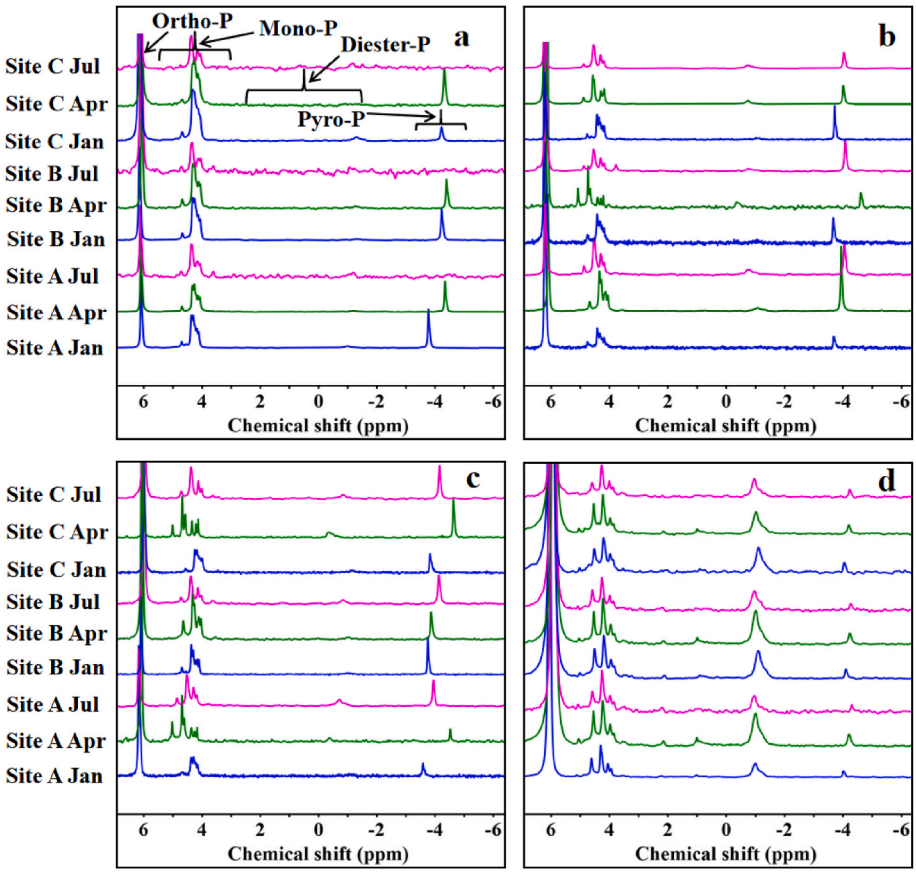

Fig. 3. ^{31}P NMR spectra of algae, SS, and sediment. Note: Panel a, b, c, and d represent algae, SS from surface water, SS from bottom water, and sediment, respectively. Ortho-P, orthophosphate; mono-P, orthophosphate monoesters; diester-P, orthophosphate diesters; pyro-P, pyrophosphate.

and pyro-P of algae extracted by NaOH-EDTA, as well as those of SS (Table S1).

3.2. P compounds extracted from algae, suspended particles, and sediment using NaOH-EDTA

Contents of NaOH-EDTA TP and their extraction ratios (calculated as NaOH-EDTA TP/TP) for all samples are shown in Fig. 2. NaOH-EDTA TP contents in algae, SS, and sediment ranged from 614 to 4042 mg kg^{-1}. The NaOH-EDTA TP extraction ratios of all samples changed dramatically (from 25.6% to 108.3%, Fig. 2), likely due to wind-wave disturbance, sediment resuspension, and SS from tributaries (Yang et al., 2020). Similar changes in NaOH-EDTA TP extraction ratios (e.g., from 42.0% to 102.0% for algae, from 51.9% to 97.4% for SS, and from 20.0% to 61.3% for sediment) have been reported previously (Shinohara et al., 2012; Feng et al., 2016; Xie et al., 2019; Yang et al., 2020).

Ortho-P, mono-P, diester-P, and pyro-P from all samples were determined by using solution ^{31}P NMR (Figs. 3 and 4, and Fig. S5−S6). Ortho-P and pyro-P were the main P_i compounds in all samples (Figs. 3 and 4). Mono-P was comprised of many compounds, which included α-glycerophosphate (4.6 ppm), β-glycerophosphate (4.3 ppm) and unknown mono-P compounds (e.g., 4.2 ppm and 3.9 ppm) (Fig. 3 and Fig. S6). Diester-P was comprised of DNA, RNA, and phospholipids (Fig. 3 and Fig. S6). Multiple peaks of mono-P and diester-P in all samples were observed in the ^{31}P NMR spectra, which highlighted their complex compounds (Fig. 3 and Fig. S6).

P compound contents and their percentages from all samples extracted by using NaOH-EDTA are shown in Fig. 4 and Fig. S5. Significant differences were observed in the contents and percentages of ortho-P and biogenic P (including mono-P, diester-P, and pyro-P, Shinohara et al., 2012) in algae, SS, and sediment (Fig. 4). The contents of ortho-P in algae (mean 1232 mg kg^{-1}) and SS (mean 1032 mg kg^{-1}) were higher than those in the sediment (mean 647 mg kg^{-1}). However, the percentages of ortho-P to their corresponding TP in algae (mean 46.8%) and SS (mean 50.6%) were lower than those in the sediment (mean 85.8%) (Fig. 4 and Fig. S5). The contents and percentages of biogenic P in algae (mean 1516 mg kg^{-1} and 53.2%) and SS (mean 945 mg kg^{-1} and 49.4%) were higher than those in the sediment (mean 105 mg kg^{-1} and 14.2%) (Fig. 4 and Fig. S5, and Table 1).

3.3. P species extracted from algae, suspended particles, and sediment using sequential extraction

Contents of P species and the percentages relative to their corresponding TP from all samples during observation are shown in Fig. 5 and Fig. S7. TP contents in algae, SS, and sediment ranged from 1441 to 7427 mg kg^{-1}. The contents and percentages of bioavailable P (including H_2O-P_i, $NaHCO_3$-P_i, and P_o) in algae (mean 2742 mg kg^{-1} and 92.8%) and SS (mean 3075 mg kg^{-1} and 81.4%) were greater than those in the sediment (mean 750 mg kg^{-1} and 37.0%) (Fig. 5 and Fig. S7). In contrast, the contents and percentages of NaOH-P_i + HCl-P_i in algae (mean 203 mg kg^{-1} and 7.2%) and SS (mean 650 mg kg^{-1} and 18.6%) were lower than those in the sediment (mean 1320 mg kg^{-1} and 63.0%) (Fig. 5 and Fig. S7).

4. Discussion

4.1. The strategies of P absorption and utilization in algae

The P absorption and utilization strategies in algae were investigated in the field. Variations of algae P_i contents (e.g., algae H_2O-P_i, algae pyro-P) and alkaline phosphatase activities during observation (Figs. 4a

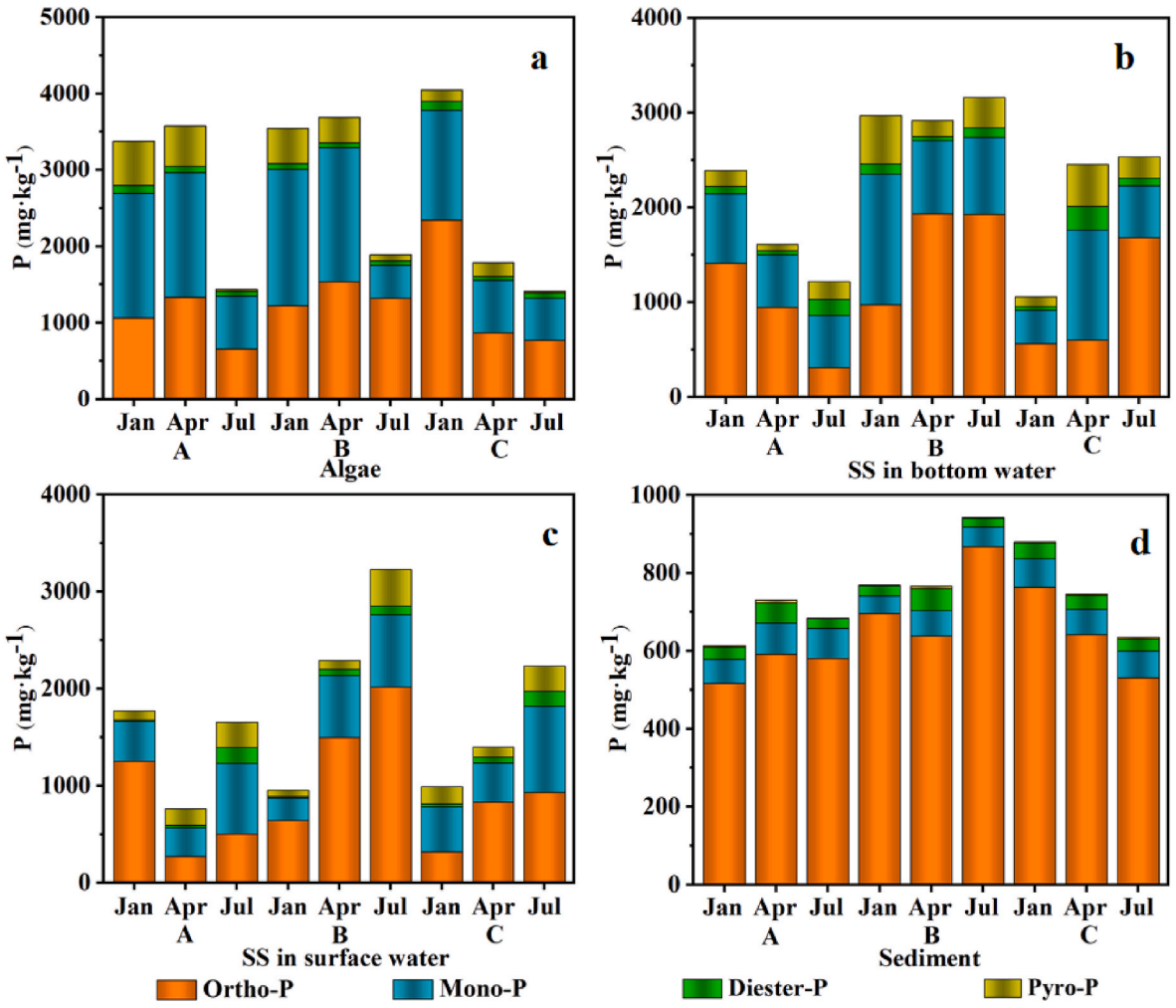

Fig. 4. Contents of P compounds in algae, SS, and sediment extracted by 0.25 M NaOH and 50 mM EDTA. Note: Panel a, b, c, and d represent algae, SS from surface water, SS from bottom water, and sediment, respectively. Ortho-P, orthophosphate; mono-P, orthophosphate monoesters; diester-P, orthophosphate diesters; pyro-P, pyrophosphate.

and 5a, and Fig. S4) demonstrated that dissolved P_i from P_o remineralization in the water column directly accumulated in algae in the form of ortho-P (e.g., H_2O-P_i) and pyro-P, especially in January (Figs. 4a and 5a). Moreover, algae preferentially utilized P_i (e.g., dissolved P_i in the water column, algae pyro-P, and algae H_2O-P_i, Figs. 4a and 5a) during growth and reproduction (e.g., January to April). And then (e.g., April to July) algae secreted more enzymes (e.g., alkaline phosphatase, Fig. S3c) to utilize P_o in the water column when these P_i was insufficient (Figs. 4a and 5a). Furthermore, alkaline phosphatase in the water column plays a vital role in regulating P supply for the growth and reproduction of algae (Fig. 5a and Fig. S3c). This fact was further supported by significantly negative correlations between P_i species of algae (e.g., H_2O-P_i, $NaHCO_3$-P_i, and NaOH-P_i) and alkaline phosphatase activities (Table S2). These results were further supported by previous indoor incubation experiments, which suggested that P_i can quickly accumulate in algae and slowly utilize during subsequent growth and reproduction (Ren et al., 2017; Feng et al., 2018; Yuan et al., 2019). The above information may be incomplete in terms of P_i released from P_o remineralization in the water column due to the absence of the phosphodiesterase activity data in this study.

4.2. Variability of P compounds in algae, suspended particles, and sediment

P released from SS can also provide P sources for algal blooms, which should be emphasized as well as sediment P. Previous studies have mainly focused on sediment P because the P released from sediment increased the P concentrations in overlying water and triggered extensive algal blooms (Chen et al., 2018; Ding et al., 2018; Yang et al., 2022). In contrast, the contents and percentages of ortho-P and biogenic P in algae and SS compared with those in the sediment (Fig. 4 and Fig. S5) demonstrated that ortho-P and biogenic P from algae and SS could be released or degraded during or after sedimentation. These results were further supported by previous laboratory simulation studies, demonstrating that the percentages of P_o hydrolyzed from algae were approximately 25 times greater than that from the sediment (Zhu et al., 2016; Feng et al., 2018).

The ratios of diester-P to mono-P can provide evidences for P cycling. With increasing P needs of algae and pressure of P supply in the water column, SS mono-P remineralization was increasingly driven by increasing alkaline phosphatase activities. Variations in ratios of diester-P to mono-P in SS (SS from surface water, Table 1), algae abundance (Fig. S4), and alkaline phosphatase activities (Fig. S3c) from January to July suggested that the faster hydrolysis rate of mono-P than that of diester-P from SS occurred to meet P needs of algae. The average ratios of diester-P to mono-P in sediment were essentially higher than those in algae and SS (Table 1), suggesting that these compounds could be degraded and regenerated during or after sedimentation. The reasonable reasons for the shift ratios are as follows: (1) The low ratios of diester-P to mono-P in algae and SS suggested that diester-P (e.g., phospholipids)

Table 1
Percentages of biogenic P and ratios of diester-P: mono-P in all samples.

Sample	sites	Time	biogenic P (%)	diester-P/mono-P
Algae	A	Jan	68.6	0.06
		Apr	62.7	0.05
		Jul	54.6	0.09
	B	Jan	65.5	0.04
		Apr	58.5	0.04
		Jul	30.4	0.13
	C	Jan	42.1	0.08
		Apr	51.3	0.07
		Jul	45.7	0.12
	Average		53.2	0.07
SS in surface water	A	Jan	29.3	0.03
		Apr	64.4	0.08
		Jul	69.8	0.23
	B	Jan	32.5	0.05
		Apr	34.6	0.10
		Jul	37.6	0.12
	C	Jan	68.0	0.06
		Apr	40.7	0.15
		Jul	58.5	0.17
	Average		48.3	0.11
SS in bottom water	A	Jan	41.0	0.11
		Apr	41.5	0.08
		Jul	74.8	0.31
	B	Jan	67.2	0.08
		Apr	33.7	0.05
		Jul	39.1	0.13
	C	Jan	47.0	0.11
		Apr	75.6	0.22
		Jul	33.7	0.14
	Average		50.3	0.14
Sediment	A	Jan	15.8	0.54
		Apr	19.0	0.64
		Jul	15.3	0.34
	B	Jan	9.4	0.59
		Apr	16.7	0.85
		Jul	8.1	0.44
	C	Jan	13.2	0.55
		Apr	14.0	0.55
		Jul	16.3	0.45
	Average		14.1	0.55

in algae and SS might have been hydrolyzed to be mono-P (e.g., α-glycerophosphate, β-glycerophosphate) (Fig. 3 and Fig. S6) during pretreatment of samples due to alkaline extraction (Turner et al., 2005; Doolette et al., 2009; Shinohara et al., 2012). Alternatively, diester-P from algae and SS *in situ* could also be naturally hydrolyzed by sunlight and phosphodiesterase (Ni et al., 2016; Li et al., 2019). (2) The observation of the increase of DNA-P in sediment probably suggested an increase in the percentage of diester-P (Fig. 3). In addition, the structure of DNA is more stable compared to RNA and phospholipids (Wang et al., 2021c). The higher ratios of diester-P to mono-P in sediment than those in the SS were further supported by a previous report, demonstrating that an increase in DNA-P in sediment could increase the corresponding ratios of diester to mono-P (Shinohara et al., 2012).

4.3. Variability of P species in algae, suspended particles, and sediment

Significant differences in the contents and percentages of bioavailable P in algae, SS, and sediment were observed (Fig. 5 and Fig. S7). In contrast to NaOH-P_i and HCl-P_i (Zhu et al., 2013; Paytan et al., 2017), H_2O-P_i, $NaHCO_3$-P_i, and P_o are generally considered as bioavailable P, which can be utilized by organisms (Zhou et al., 2000; Zhu et al., 2013; Ni et al., 2016; Feng et al., 2018). The lower contents and percentages of bioavailable P in sediment than those in algae and SS reflected that most of bioavailable P was released or degraded during or after sedimentation (Fig. 5 and Fig. S7). In contrast, the high contents of P_o (mean 1066 mg kg^{-1}) and their corresponding percentages (mean 33.8%) in all samples (Fig. 5 and Fig. S7) suggested that most of the P_o was contributed by algae or algae debris (Feng et al., 2020). As algae is an important component of SS, which increase the contents of SS P_o. A high sediment P_o content was also observed, which can be attributed to algae debris. Similar results have been reported for P_o in algae and sediment in the same research area of Lake Dianchi. For example, the contents of P_o in algae and sediment were up to 3646 mg kg^{-1} and 1347 mg kg^{-1}, respectively, accounting for 70% and 56% of TP (Xie et al., 2019). Furthermore, the contents of particular organic P (POP) ranged from 126 to 1026 μmol g^{-1} (3906–31806 mg kg^{-1}) in a hypereutrophic freshwater estuary, and the percentages of POP to total particular P (TPP) ranged from 47% to 87% (Yang et al., 2021).

Variation of algae P_i might be controlled by the P absorption and utilization strategies of algae. Unlike the irregular variations in the contents of P_i species in SS from January to July, the contents of P_i species of algae in these periods gradually decreased (especially algae H_2O-P_i, Fig. 5). The variations of P_i species in algae during growth and reproduction were likely attributed to its P absorption and utilization strategies (see section 4.1). Additionally, algal blooms led to increase algae P needs, as reflected by the lowest algae P_i content in July (Fig. 5a and Fig. S4). Moreover, the greater P_i contents of SS than that of algae in July suggested the possibility of competition between algae and SS for dissolved P_i in the water column (Fig. 5a and b). Consequently, increasing the pressure of P supply from water column may lead algae to increasingly rely on P_o remineralization to meet its P needs. This proposition was further supported by the increase of alkaline phosphatase activities in July (Fig. S3c). As for P_i species of SS, the possible factors included the mineral compositions of SS and SS concentrations (River and Richardson, 2018; Ji et al., 2022; Walch et al., 2022). More evidences of the SS compositions and the ability of P absorbed by SS are needed in ongoing work.

5. Conclusions

This study suggested that P released from SS provide important P sources for algal blooms. Dissolved P_i in the water column directly accumulated in algae. Algae preferentially utilized P_i and subsequently utilized P_o in the water column when the P_i was insufficient. Alkaline phosphatase in the water column plays a key role in regulating the P supply for algae during growth and reproduction. Ortho-P, mono-P, diester-P, and pyro-P in all samples were identified by solution ^{31}P NMR. Ortho-P and biogenic P were the main P compounds in algae and SS, and ortho-P was the main P compound in sediment. SS mono-P remineralization was increasingly driven by increasing alkaline phosphatase activities, which was attributed to increasing P needs of algae and pressure of P supply in the water column. The higher ratios of diester-P to mono-P in sediment than those in the algae and SS suggested that the degradation and regeneration occurred within these P compounds during or after sedimentation. H_2O-P_i, $NaHCO_3$-P_i, and P_o were the main P species in algae and SS, whereas NaOH-P_i and HCl-P_i were the main P species in sediment. Contents of P_i in algae during growth and reproduction were controlled by its P absorption and utilization strategies. These results emphasize the high contribution of labile P from SS to sustain algal blooms in Lake Dianchi, which provides critical information on the understanding of algal blooms in the surface water with low concentrations of dissolved P and designment of appropriate nutrient management strategies.

Credit author statement

Zuxue Jin: Investigation, Formal analysis, Data curation, Writing – original draft. Jingfu Wang: Conceptualization, Methodology, Writing – review & editing, Project administration. Shihao Jiang: Investigation, Formal analysis. Jiaojiao Yang: Investigation, Formal analysis, Data curation. Shuoru Qiu: Investigation, Data curation. Jingan Chen: Methodology, Writing – review & editing, Project administration.

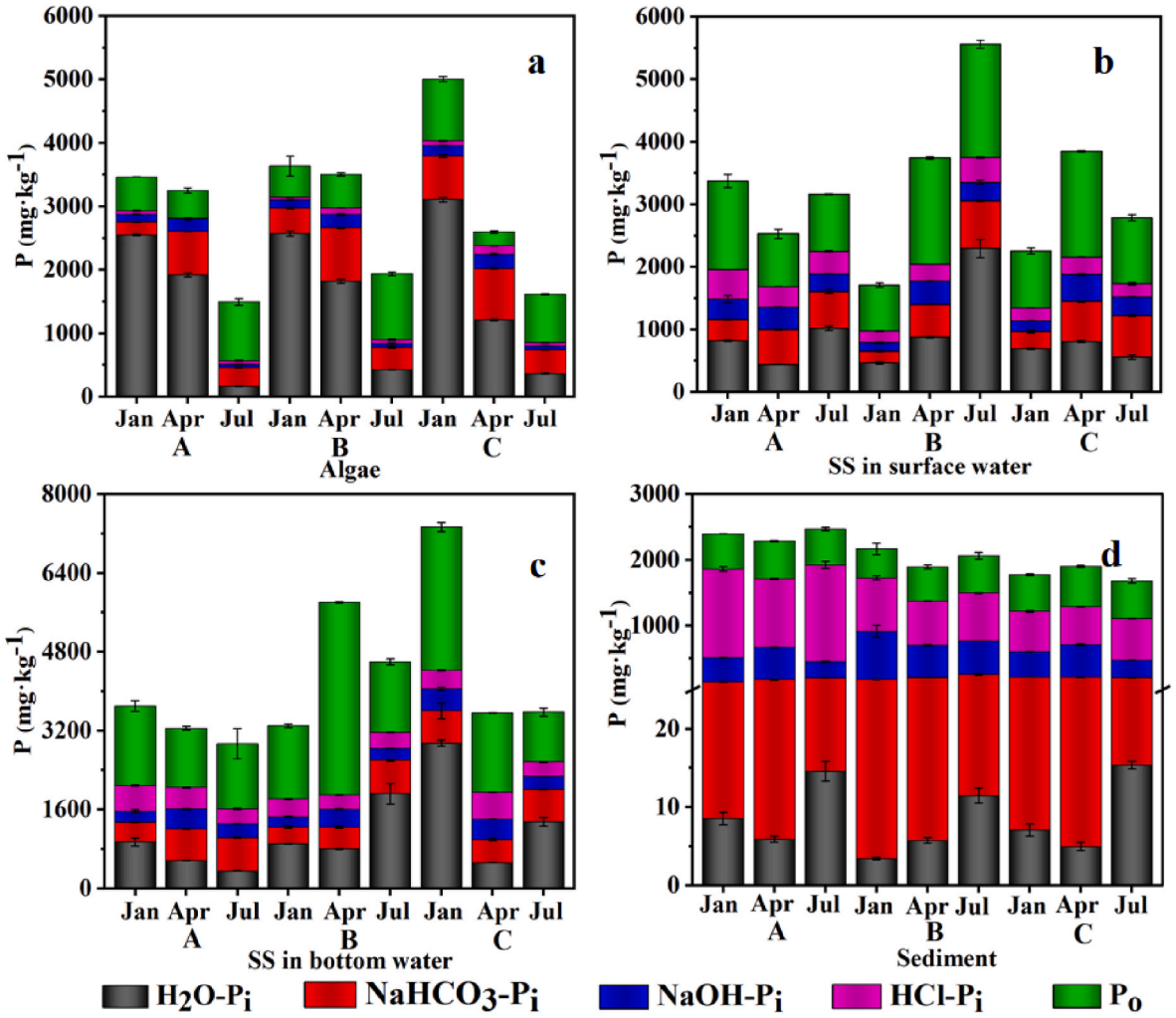

Fig. 5. Contents of P species in algae, SS, and sediment extracted by modified Hedley' method. Note: Panel a, b, c, and d represent algae, SS from surface water, SS from bottom water, and sediment, respectively. Error bar represents standard deviations of triplicated measurements. Where error bars are not visible, they are smaller than the data symbols.

Declaration of competing interest

The authors declare that they have no known competing financial interests or personal relationships that could have appeared to influence the work reported in this paper.

Data availability

Data will be made available on request.

Acknowledgements

This study was sponsored jointly by the Strategic Priority Research Program of CAS (No. XDB40020400), the National Key R&D Plan of China (2021YFC3201000), the Science and Technology Service Plan of CAS (KFJSTSQYZD202124001), the Central Leading Local Science and Technology Development Fund Project (20214028), the Chinese NSF Project (No. 41773145, 41977296), the Youth Innovation Promotion Association CAS (No. 2019389), and the CAS Interdisciplinary Innovation Team.

Appendix A. Supplementary data

Supplementary data to this article can be found online at https://doi.org/10.1016/j.envpol.2022.119964.

References

Ahlgren, J., Reitzel, K., Danielsson, R., Gogoll, A., Rydin, E., 2006. Biogenic phosphorus in oligotrophic mountain lake sediments: Differences in composition measured with NMR spectroscopy. Water Res. 40, 3705–3712.

Aspila, K., Agemian, H., Chau, A., 1976. A semi-automated method for the determination of inorganic, organic, and total phosphate in sediments. The Analyst. 101, 187–197.

Bai, X.L., Sun, J.H., Zhou, Y.K., Gu, L., Zhao, H.Y., Wang, J.H., 2017. Variations of different dissolved and particulate phosphorus classes during an algae bloom in a eutrophic lake by ^{31}P NMR spectroscopy. Chemosphere. 169, 577–585.

Boon, P.I., 1989. Organic matter degradation and nutrient regeneration in Australian freshwaters: I. methods for exoenzyme assays in turbid aquatic environments. Arch. Hydrobiol. 115 (3), 339–359.

Cade-Menun, B.J., 2005. Characterizing phosphorus in environmental and agricultural samples by ^{31}P nuclear magnetic resonance spectroscopy. Talanta. 66, 359–371.

Cade-Menun, B.J., Preston, C.M., 1996. A comparison of soil extraction procedures for ^{31}P NMR spectroscopy. Soil Sci. 161, 770–785.

Chen, M.S., Ding, S.M., Chen, X., Sun, Q., Fan, X.F., Lin, J., Ren, M.Y., Yang, L.Y., Zhang, C.S., 2018. Mechanisms driving phosphorus release during algal blooms based on hourly changes in iron and phosphorus concentrations in sediments. Water Res. 133, 153–164.

Ding, S.M., Chen, M.S., Gong, M.D., Fan, X.F., Qin, B.Q., Xu, H., Gao, S.S., Jin, Z.F., Tsang, D.C.W., Zhang, C.S., 2018. Internal phosphorus loading from sediments causes seasonal nitrogen limitation for harmful algal blooms. Sci. Total Environ. 625, 872–884.

Doolette, A.L., Smernik, R.J., Dougherty, W.J., 2009. Spiking improved solution phosphorus-31 nuclear magnetic resonance identification of soil phosphorus compounds. Soil Sci. Soc. Am. J. 73 (3), 919.

Feng, W.Y., Zhu, Y.R., Wu, F.C., He, Z.Q., Zhang, C., Giesy, J.P., 2016. Forms and lability of phosphorus in algae and aquatic macrophytes characterized by solution ^{31}P NMR coupled with enzymatic hydrolysis. Sci. Rep. 6, 37164.
Feng, W.Y., Wu, F.C., He, Z.Q., Song, F.H., Zhu, Y.R., Giesy, J.P., Wang, Y., Qin, N., Zhang, C., Chen, H.Y., Sun, F.H., 2018. Simulated bioavailability of phosphorus from aquatic macrophytes and phytoplankton by aqueous suspension and incubation with alkaline phosphatase. Sci. Total Environ. 616–617, 1431–1439.
Feng, W.Y., Yang, F., Zhang, C., Liu, J., Song, F.H., Chen, H.Y., Zhu, Y.R., Liu, S.S., Giesy, J.P., 2020. Composition characterization and biotransformation of dissolved, particulate and algae organic phosphorus in eutrophic lakes. Environ. Pollut. 265, 114838.
Gage, M.A., Gorham, E., 1985. Alkaline phosphatases activity and cellular phosphorus as an index of the phosphorus status of phytoplankton in Minnesota lakes. Freshw. Biol. 15 (2), 227–233.
Gao, W., Cheng, G.W., Yan, C.A., Chen, Y., 2021. Identifying spatiotemporal alteration of nitrogen to phosphorus ratio of Lake Dianchi and its driving forces during 1988-2018. J. Lake Sci. 33 (1), 64–73 (In Chinese).
He, Z.J., Xiong, Q., Jiao, L.X., Wang, S.R., 2014. Characteristics and bioavailability of dissolved organic phosphorus from different sources of Lake Dianchi in summer. China Environ. Sci. 34, 3189–3198 (In Chinese).
Hedley, M.J., Stewart, J.W.B., Chauhan, B.S., 1982. Changes in inorganic and organic soil phosphorus fractions induced by laboratory incubations. Soil Sci. Soc. Am. J. 46, 970–976.
Hu, H.J., Wei, Y.X., 2006. The Freshwater Algae of China: Systematics, Taxonomy and Ecology. Science Press, Beijing.
Huang, X.F., Chen, W.M., Cai, Q.M., 1999. Standard Methods for Observation and Analysis in Chinese Technology of Lake Ecology. Standards press of China, Beijing.
Ji, N.N., Liu, Y., Wang, S.R., Wu, Z.H., Li, H., 2022. Buffering effect of suspended particulate matter on phosphorus cycling during transport from rivers to lakes. Water Res. 216, 118350.
Li, W., Joshi, S.R., Hou, G.J., Burdige, D.J., Sparks, D.L., Jaisi, D.P., 2015. Characterizing phosphorus speciation of Chesapeake Bay sediments using chemical extraction, ^{31}P NMR, and X-ray absorption fine structure spectroscopy. Environ. Sci. Technol. 49, 203–211.
Li, X.L., Guo, M.L., Duan, X.D., Zhao, J.W., Hua, Y.M., Zhou, Y.Y., Liu, G.L., Dionysiou, D. D., 2019. Distribution of organic phosphorus species in sediment profiles of shallow lakes and its effect on photo-release of phosphate during sediment resuspension. Environ. Int. 130, 104916.
Liu, Y., Wang, J.F., Chen, J.A., Zhang, R.Y., Ji, Y.X., Jin, Z.X., 2019. Pretreatment method for the analysis of phosphate oxygen isotope ($\delta^{18}O_P$) of different phosphorus fractions in freshwater sediments. Sci. Total Environ. 685, 229–238.
Ma, X.X., Wang, Y.N., Feng, S.Q., Wang, S.B., 2015. Vertical migration patterns of different phytoplankton species during a summer bloom in Dianchi Lake, China. Environ. Earth Sci. 74, 3805–3814.
Murphy, J., Riley, J.P., 1962. A modified single solution method for the determination of phosphate in natural waters. Anal. Chim. Acta. 26, 31–36.
Ni, Z.K., Wang, S.R., Wang, Y.M., 2016. Characteristics of bioavailable organic phosphorus in sediments and its contribution to lake eutrophication in China. Environ. Pollut. 219, 537–544.
Paytan, A., Roberts, K., Watson, S., Peek, S., Chuang, P.C., Defforey, D., Kendall, C., 2017. Internal loading of phosphate in Lake Erie Central Basin. Sci. Total Environ. 579, 1156–1165.
Ren, L.X., Wang, P.F., Wang, C., Chen, J., Hou, J., Qian, J., 2017. Algal growth and utilization of phosphorus studied by combined mono-culture and co-culture experiments. Environ. Pollut. 220, 274–285.
River, M., Richardson, C., 2018. Stream transport of iron and phosphorus by authigenic nanoparticles in the Southern Piedmont of the. U.S. Water Res. 130, 312–321.
Shinohara, R., Imai, A., Kawasaki, N., Komatsu, K., Kohzu, A., Miura, S., Sano, T., Tomioka, N., 2012. Biogenic phosphorus compounds in sediment and suspended particles in a shallow eutrophic lake: A ^{31}P-nuclear magnetic resonance (^{31}P NMR) study. Environ. Sci. Technol. 46, 10572–10578.
Tang, X.Q., Wu, M., Li, R., 2018. Distribution, sedimentation, and bioavailability of particulate phosphorus in the mainstream of the Three Gorges Reservoir. Water Res. 140, 44–55.
Turner, B.L., Cade-Menun, B.J., Westermann, D.T., 2003. Organic phosphorus composition and potential bioavailability in semi-arid arable soils of the western United States. Soil Sci. Soc. Am. J. 67, 1168–1179.
Turner, B.L., Frossard, E., Baldwin, D.S., 2005. Organic Phosphorus in the Environment. CABI Publishing, New South Wales, Australia.
Walch, H., von der Kammer, F., Hofmann, T., 2022. Freshwater suspended particulate matter-key components and processes in floc formation and dynamics. Water Res. 220, 118655.
Wang, J.H., He, L.Q.S., Yang, C., Dao, G.H., Du, J.S., Han, Y.P., Wu, G.X., Wu, Q.Y., Hu, H.Y., 2018. Comparison of algal bloom related meteorological and water quality factors and algal bloom conditions among Lakes Taihu, Chaohu, and Dianchi (1981-2015). J. Lake Sci. 30 (4), 897–906 (In Chinese).
Wang, C.Y., Yang, Y.Y., Yang, B., Lin, H., Miller, T.R., Newton, R.J., Guo, L.D., 2021a. Causal relationship between alkaline phosphatase activities and phosphorus dynamics in a eutrophic coastal lagoon in Lake Michigan. Sci. Total Environ. 787, 147682.
Wang, J.H., Li, C., Xu, Y.P., Li, S.Y., Du, J.S., Han, Y.P., Hu, H.Y., 2021b. Identifying major contributors to algal blooms in Lake Dianchi by analyzing river-laker water quality correlations in the watershed. J. Clean. Prod. 315, 128144.
Wang, L.M., Amelung, W., Willbold, S., 2021c. ^{18}O isotope labeling combined with ^{31}P nuclear magnetic resonance spectroscopy for accurate quantification of hydrolysable phosphorus species in environmental samples. Anal. Chem. 93, 2018–2025.
Wu, Z., Liu, Y., Liang, Z.Y., Wu, S.F., Guo, H.C., 2017. Internal cycling, not external loading, decides the nutrient limitation in eutrophic lake: A dynamic model with temporal Bayesian hierarchical inference. Water Res. 116, 231–240.
Xie, F.Z., Li, L., Song, K., Li, G.L., Wu, F.C., Giesy, J.P., 2019. Characterization of phosphorus forms in a eutrophic lake, China. Sci. Total Environ. 659, 1437–1447.
Yang, P., Yang, C.H., Yin, H.B., 2020. Dynamics of phosphorus composition in suspended particulate matter from a turbid eutrophic shallow lake (Lake Chaohu, China): Implications for phosphorus cycling and management. Sci. Total Environ. 741, 140203.
Yang, B., Lin, H., Bartlett, S.L., Houghton, E.M., Robertson, D.M., Guo, L.D., 2021. Partitioning and transformation of organic and inorganic phosphorus among dissolved, colloidal and particulate phases in a hypereutrophic freshwater estuary. Water Res. 196, 117025.
Yang, C.H., Li, J.Y., Yin, H.B., 2022. Phosphorus internal loading and sediment diagenesis in a large eutrophic lake (Lake Chaohu, China). Environ. Pollut. 292, 118471.
Yu, J., Chen, J.A., Zeng, Y., Lu, Y.T., Chen, Q., 2020. Carbon and phosphorus transformation during the deposition of particulate matter in the large deep reservoir. J. Environ. Manag. 265, 110514.
Yuan, R.Y., Li, J.H., Li, Y., Ren, L., Wang, S., Kong, F.L., 2019. Formation mechanism of the *Microcystis aeruginosa* bloom in the water with low dissolved phosphorus. Mar. Pollut. Bull. 148, 194–201.
Zhang, Y., Zuo, J.N., Salimova, A., Li, A.J., Li, L., Li, D., 2020. Phytoplankton distribution characteristics and its relationship with bacterioplankton in Dianchi Lake. Environ. Sci. Pollut. Res. 27, 40592–40603.
Zhou, Q.X., Gibson, C.E., Zhu, Y.M., 2000. Evaluation of phosphorus bioavailability in sediments of three contrasting lakes in China and the UK. Chemosphere 42, 221–225.
Zhu, Y.R., Wu, F.C., He, Z.Q., Guo, J.Y., Qu, X.X., Xie, F.Z., Giesy, J.P., Liao, H.Q., Guo, F., 2013. Characterization of organic phosphorus in lake sediments by sequential fractionation and enzymatic hydrolysis. Environ. Sci. Technol. 47, 7679–7687.
Zhu, Y.R., Wu, F.C., Feng, W.Y., Liu, S.S., Giesy, J.P., 2016. Interaction of alkaline phosphatase with minerals and sediments: activities, kinetics and hydrolysis of organic phosphorus. Colloid. Surface. A. 495, 46–53.